Calsyntenin-1 shelters APP from proteolytic processing during anterograde axonal transport

Martin Steuble[1], Tu-My Diep[1], Philipp Schätzle[1], Alexander Ludwig[1], Mitsuo Tagaya[2], Beat Kunz[1] and Peter Sonderegger[1,*]

[1]Department of Biochemistry, University of Zurich, Winterthurerstrasse 190, CH-8057 Zurich, Switzerland
[2]Tokyo University of Pharmacy and Life Science, Hachioji, Tokyo 192-0392, Japan
*Author for correspondence (Peter.Sonderegger@bioc.uzh.ch)

Biology Open 1, 761–774
doi: 10.1242/bio.20121578
Received 5th April 2012
Accepted 22nd May 2012

Summary

Endocytosis of amyloid-β precursor protein (APP) is thought to represent the major source of substrate for the production of the amyloidogenic Aβ peptide by the β-secretase BACE1. The irreversible nature of proteolytic cleavage implies the existence of an efficient replenishment route for APP from its sites of synthesis to the cell surface. We recently found that APP exits the *trans*-Golgi network in intimate association with calsyntenin-1, a transmembrane cargo-docking protein for Kinesin-1-mediated vesicular transport. Here we characterized the function of calsyntenin-1 in neuronal APP transport using selective immunoisolation of intracellular trafficking organelles, immunocytochemistry, live-imaging, and RNAi. We found that APP is co-transported with calsyntenin-1 along axons to early endosomes in the central region of growth cones in carriers that exclude the α-secretase ADAM10. Intriguingly, calsyntenin-1/APP organelles contained BACE1, suggesting premature cleavage of APP along its anterograde path. However, we found that APP contained in calsyntenin-1/APP organelles was stable. We further analyzed vesicular trafficking of APP in cultured hippocampal neurons, in which calsyntenin-1 was reduced by RNAi. We found a markedly increased co-localization of APP and ADAM10 in axons and growth cones, along with increased proteolytic processing of APP and Aβ secretion in these neurons. This suggested that the reduced capacity for calsyntenin-1-dependent APP transport resulted in mis-sorting of APP into additional axonal carriers and, therefore, the premature encounter of unprotected APP with its ectodomain proteases. In combination, our results characterize calsyntenin-1/APP organelles as carriers for sheltered anterograde axonal transport of APP.

Key words: APP, Anterograde axonal transport, Calsyntenin-1, Alzheimer's disease, Amyloid β, α-secretase, β-secretase, ADAM10, BACE1

Introduction

Excessive production of pathogenic amyloid-β (Aβ) peptide from amyloid-β precursor protein (APP) is considered as the biochemical hallmark of Alzheimer's disease (Haass and Selkoe, 2007). Aβ formation requires proteolytic cleavage of APP in the juxtamembrane region of its ectodomain by the β-secretase BACE1, followed by intramembrane cleavage by γ-secretase. Competing ectodomain cleavage within the Aβ segment of APP by α-secretase, followed by intramembrane cleavage by γ-secretase, produces the non-amyloidogenic p3 peptide and, thereby, precludes Aβ formation (Sisodia, 1992a). APP has been found at the plasma membrane and, for a fraction of it, internalization through endocytosis and recycling back to the cell surface have been reported (Haass et al., 1992; Koo et al., 1996; Yamazaki et al., 1996; Marquez-Sterling et al., 1997; Groemer et al., 2011). Along its recycling itinerary, APP may be cleaved by α-secretase at the plasma membrane (Sisodia, 1992b; Kojro and Fahrenholz, 2005) and by β-secretase in the early endosome (EE) (Koo and Squazzo, 1994; Perez et al., 1999; Grbovic et al., 2003; Kinoshita et al., 2003; Carey et al., 2005; Rajendran et al., 2006; Small and Gandy, 2006; He et al., 2007). Based on these findings it is now widely accepted that EEs are a major site of β-secretase activity and that APP internalized from the plasma membrane plays an essential role in Aβ generation. Accordingly, targeted inhibition of endosomal BACE1 through a transition-state inhibitor linked to a sterol was recently shown to reduce Aβ production *in vitro* and *in vivo* (Rajendran et al., 2008).

In neurons, the presynaptic nerve is a major site for the release of the soluble ectodomain of APP after proteolytic cleavage by α-secretase (sAPPα) (Nitsch et al., 1992). The irreversible nature of proteolytic processing requires continuous replenishment of APP by anterograde axonal transport. Already two decades ago kinesin was identified as the main molecular motor required for the transport of APP-containing vesicles (Koo et al., 1990; Ferreira et al., 1993; Kaether et al., 2000). Yet, the molecular components and interactions that mediate the connection between APP-containing transport vesicles and Kinesin-1 motors are still controversial. A direct, high-affinity interaction between the cytoplasmic segment of APP and the tetratricopeptide repeat region of the light chains of Kinesin-1 was proposed based on immunoprecipitations (Kamal et al., 2000). An indirect

connection between APP and Kinesin-1 motors was proposed based on reports that c-Jun N-terminal kinase-interacting protein 1 (JIP1b) would act as a bridging protein by simultaneously binding both APP and kinesin light chain-1 (Matsuda et al., 2003; Inomata et al., 2003). However, both mechanisms were questioned by subsequent work by several independent labs that failed to reproduce the direct binding between APP and Kinesin-1 (Lazarov et al., 2005) and the fact that absence of JIP1b did not affect transport of APP (Kins et al., 2006). These objections were backed by a series of reports indicating that APP variants lacking the cytoplasmic segment were still efficiently delivered to axons in several distinct model systems of axonal transport (Tienari et al., 1996; Torroja et al., 1999; Rusu et al., 2007; Back et al., 2007; Szodorai et al., 2009). These results, together with the recent observation that distinct forms of APP are independently transported in separate carrier vesicles (Muresan et al., 2009), suggest that further scrutiny is required to resolve the detailed mechanism(s) of anterograde axonal transport of APP.

We recently found that APP exits the trans-Golgi network (TGN) in intimate association with calsyntenin-1, a transmembrane cargo-docking protein for Kinesin-1-mediated anterograde axonal transport of membrane-bounded organelles (Vogt et al., 2001; Hintsch et al., 2002; Konecna et al., 2006; Ludwig et al., 2009). Like APP, calsyntenin-1 is subject to two-step proteolytic processing. After the first cleavage in the juxtamembrane region of its ectodomain (Vogt et al., 2001), the C-terminal fragment of calsyntenin-1 is cleaved within its transmembrane segment by γ-secretase (Araki et al., 2003). A recent study indicates that the α-secretases ADAM10 and ADAM17, but not the β-secretase BACE1, are capable of cleaving calsyntenin-1's ectodomain (Hata et al., 2009).

Using organelle immunoisolation and proteomics, we recently demonstrated that calsyntenin-1 organelles contain components characteristic of vesicles of endosomal pathways (Steuble et al., 2010). Axons contained at least two distinct, non-overlapping calsyntenin-1-containing transport packages, one characterized by the presence of APP and early-endosomal markers (Rab5), the other with recycling-endosomal markers (Rab11) and no APP (Steuble et al., 2010). In accordance with the identification of calsyntenin-1/APP vesicles as a distinctive carrier for anterograde axonal transport of APP we found that calsyntenin-1 and APP exit the TGN together in a vesicle with early-endosomal characteristics (Ludwig et al., 2009) and that all calsyntenin-1 vesicles are transported anterogradely along axons (Konecna et al., 2006). RNAi studies in cultured neurons indicated that down-regulation of calsyntenin-1 results in enhanced APP processing (Ludwig et al., 2009; Vagnoni et al., 2012). Based on the observation of reduced levels of calsyntenin-1 in brains of humans affected with Alzheimer's disease a pathogenic role of calsyntenin-1 dysfunction and Alzheimer's disease was suggested (Vagnoni et al., 2012).

Here we set out to characterize the role of calsyntenin-1 and calsyntenin-1-containing vesicles in axonal APP transport and proteolytic processing. Because work of several laboratories located proteolytic processing of APP by α- and β-secretases in the axonal periphery, we wondered whether anterograde axonal transport of full-length APP included mechanisms to protect APP from its processing proteases during transport to its peripheral destination. The β-secretase has been unequivocally identified as the aspartyl protease BACE1 over a decade ago (Vassar, 2004). In contrast, the molecular identity of α-secretase has long remained controversial. The most frequently discussed candidates were members of the ADAM (a disintegrin and metalloprotease) family, ADAM9, ADAM10, and ADAM17 (Koike et al., 1999; Lammich et al., 1999; Slack et al., 2001). However, studies over the past decade have accumulated evidence that the physiologically most relevant α-secretase responsible for APP processing in the brain is ADAM10 (Kuhn et al., 2010; Jorissen et al., 2010). The role of ADAM9 in α-secretase cleavage of APP was discredited mainly by its failure to cleave an APP-derived peptide at the α-cleavage site *in vitro* (Roghani et al., 1999) and the finding that α-secretase-derived cleavage products of APP were not reduced in mice lacking ADAM9 (Weskamp et al., 2002). ADAM17 was shown to be mainly expressed in astrocytes and endothelial cells, but not in neurons (Goddard et al., 2001) and, in accordance with this observation, we did not find ADAM17 in immunoisolated calsyntenin-1 vesicles (supplementary material Fig. S1).

We show here that calsyntenin-1/APP organelles that are cotransported anterogradely along axons contain BACE1, but no ADAM10, both at the level of the growth cone and along the axon. The presence of BACE1 raised speculations about a premature cleavage of APP along its anterograde axonal path. However, incubation studies with immunoisolated vesicles indicated that APP contained in calsyntenin-1/APP organelles was stable, implying that calsyntenin-1 provides a protective mechanism for axonal transport of APP. After arrival in endosomes of the growth cone, APP may be released from its protective complex via cleavage of calsyntenin-1 by endocytosed ADAM10.

Results

BACE1, but not ADAM10, is present in calsyntenin-1/APP organelles

Full-length APP that is lost by proteolytic cleavage during its local recycling in the growth cone may be replenished by calsyntenin-1-dependent anterograde delivery of APP to EEs of growth cones (Steuble et al., 2010). To further characterize the axonal calsyntenin-1/APP carrier, we immunoisolated calsyntenin-1, APP, syntaxin13, Rab11, and Rab5 vesicles and tested them for the presence of ADAM10 and BACE1 (Fig. 1A–E). Conversely, we immunoisolated ADAM10 and BACE1 organelles with antibodies directed against cytoplasmic epitopes of ADAM10 and BACE1, respectively, and tested them for their content of calsyntenin-1, APP, as well as a series of established organelle markers (Fig. 1F,G). Organelle immunoisolations were performed with specific antibodies against marker proteins and magnetic Dynabeads M-280 decorated with anti-IgG (Fig. 1A). Protocol and specificity of the previously established immunoisolations of calsyntenin-1, syntaxin13, Rab11, and Rab5 organelles were reported previously (Steuble et al., 2010). The specificity of the immunoisolations of APP, ADAM10, and BACE1 organelles is demonstrated in Fig. 1B. Calsyntenin-1 immunoisolates contained BACE1, but not ADAM10 (Fig. 1C, boxed). In contrast, APP, syntaxin13, and Rab5 immunoisolates contained both BACE1 and ADAM10 (Fig. 1D,E, boxed), while Rab11 immunoisolates were devoid of both (Fig. 1D, boxed). Because Rab11 immunoisolates did not contain BACE1, we concluded that BACE1 was selectively associated with early-endosomal calsyntenin-1/APP carriers. The absence of ADAM10 from calsyntenin-1 immunoisolates indicated separate

anterograde axonal transport for ADAM10 and calsyntenin-1-associated APP.

Separate trafficking of ADAM10 and calsyntenin-1-associated APP was corroborated by the absence of calsyntenin-1 from ADAM10 immunoisolates (Fig. 1F, black box). Because ADAM10 immunoisolates did not contain Rab11 (Fig. 1F) and Rab11 immunoisolates did not contain ADAM10 (Fig. 1D, boxed), we concluded that ADAM10 was also absent from early endosomes (REs) of the slow recycling route. Together, these results indicated that ADAM10 is transported by a calsyntenin-1-free organelle, presumably on a secretory route.

ADAM10 is a resident of early endosomes

Besides the expected plasma-membrane marker syntaxin4 (Fig. 1F, green box), ADAM10 immunoisolates also contained the EE marker Rab5 and the pan-endosomal marker syntaxin13

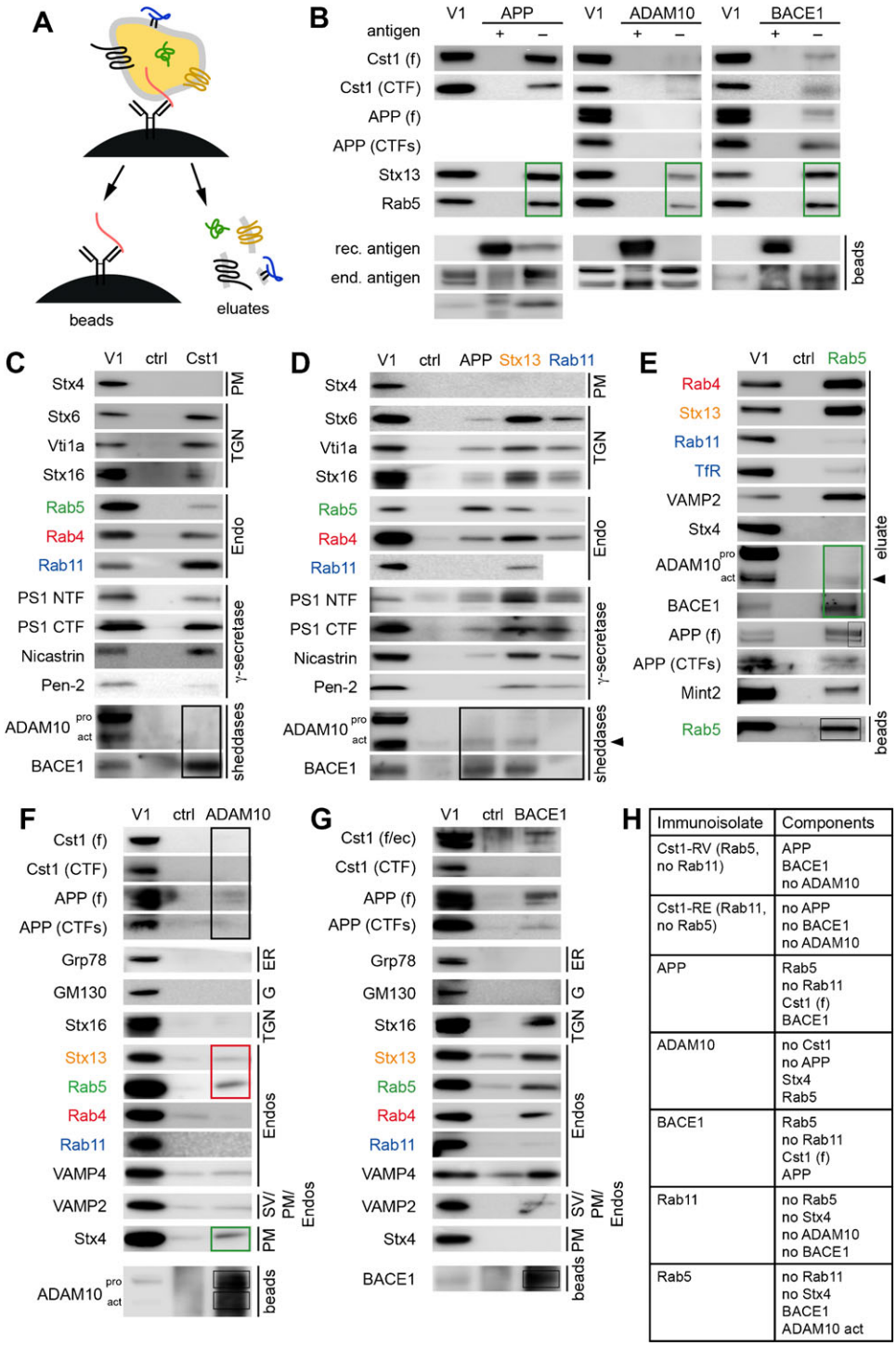

H

Immunoisolate	Components
Cst1-RV (Rab5, no Rab11)	APP BACE1 no ADAM10
Cst1-RE (Rab11, no Rab5)	no APP no BACE1 no ADAM10
APP	Rab5 no Rab11 Cst1 (f) BACE1
ADAM10	no Cst1 no APP Stx4 Rab5
BACE1	Rab5 no Rab11 Cst1 (f) APP
Rab11	no Rab5 no Stx4 no ADAM10 no BACE1
Rab5	no Rab11 no Stx4 BACE1 ADAM10 act

Fig. 1. See next page for legend.

(Fig. 1F, red box). Conversely, Rab5 immunoisolates contained active ADAM10 (Fig. 1E, green box), but were devoid of syntaxin4. The absence of plasma-membrane components from our Rab5-based preparations of EEs implies that ADAM10 is present in EEs (Fig. 1E). As Western blots showed active ADAM10, but not its pro-form in syntaxin 13 and Rab5 immunoisolates (Fig. 1D,E, arrowhead), we further concluded that ADAM10 reaches EEs upon activation at the plasma membrane and subsequent endocytosis, rather than by direct delivery to EEs on an anterograde route.

BACE1 colocalizes with APP in anterogradely transported axonal calsyntenin-1/APP organelles

BACE1 immunoisolates contained calsyntenin-1, APP, the pan-endosomal marker syntaxin13, as well as the EE marker Rab5, but not the RE marker Rab11 (Fig. 1G). Therefore, we concluded that BACE1 immunoisolates comprised a substantial fraction of early-endosomal vesicles. This is further supported by the abundance of BACE1 in Rab5 immunoisolates (Fig. 1E, green box).

To localize BACE1-containing vesicles in axons and growth cones, we performed double-staining of dissociated hippocampal neurons after 4 DIV with antibodies against calsyntenin-1, APP, syntaxin13, and the RE marker Rip11. We used an antibody against Rip11, a Rab11-binding protein, as a substitute marker for Rab11, because we could not find a suitable anti-Rab11 antibody for immunocytochemistry. Axons were distinguished from dendrites by staining for hypo-phosphorylated Tau-1 (Kempf et al., 1996). As documented in Fig. 2, we found a strong colocalization of BACE1 with calsyntenin-1, APP, and syntaxin13 both along axons and in the C-domain of growth cones, while considerably less overlap was found in the P-domain of growth cones (Fig. 2A, a1–c4; Fig. 2B, a1–c4; Fig. 2C–E). The fractions of Rip11 vesicles containing BACE1 were low (2–5%) in all regions examined (Fig. 2A, d1–d4; Fig. 2B, d1–d4; Fig. 2C–E).

The reduction of BACE1 from calsyntenin-1, APP, and syntaxin13 puncta at the transition from the C- to the P-region is consistent with the notion that axonally transported BACE1 accumulates in EEs and that EEs are the main site of BACE1 action (Koo and Squazzo, 1994; Perez et al., 1999; Kinoshita et al., 2003; Rajendran et al., 2006; Rajendran et al., 2008; He et al., 2007). In summary, the distribution pattern of BACE1 along the axon and in the growth cones strongly resembled that of early-endosomal calsyntenin-1/APP organelles. In contrast, only very little colocalization of BACE1 with Rip11 was found.

To corroborate the association of BACE1 with the anterograde trajectory of axonal calsyntenin-1/APP/BACE1 vesicles we expressed combinations of fluorescently tagged calsyntenin-1, APP, BACE1 in cultured hippocampal neurons and tracked their vesicular migration along axons by live-imaging. Anterograde tracks clearly outnumbered retrograde tracks for all tested components and the tagged molecules co-localized in most of the tracks (Fig. 3A–C). Approximately 73% of calsyntenin-1-eGFP, 69% of calsyntenin-1-mRFP, 74% of APP-mRFP, and 72% of BACE1-eGFP transport packages moved in anterograde direction. Likewise, 77% of calsyntenin-1/APP, 69% of calsyntenin-1/BACE, and 69% of APP/BACE vesicles were associated with anterograde tracks (Fig. 3D–F). These results indicated that a substantial fraction of APP and its β-secretase BACE1 are co-transported anterogradely along axons in calsyntenin-1/APP-positive carriers to EEs in the C-domain of growth cones.

Calsyntenin-1 of the anterograde axonal calsyntenin-1/APP route is proteolytically degraded in early endosomes in the C-region of the growth cone

We previously speculated that early-endosomal, APP-positive and Rab11-negative calsyntenin-1 transport packages cease their anterograde axonal trajectory in EEs of growth cones through proteolytic cleavage of calsyntenin-1 (Steuble et al., 2010). To test this hypothesis, we analyzed syntaxin13, APP, and Rab11 immunoisolates for calsyntenin-1 cleavage products before and after incubation at 37℃ for 30 min under conditions that preserve their luminal pH and analyzed calsyntenin-1 processing using Western blotting (Fig. 4A–G). Calsyntenin-1 remained unaltered during incubation of APP immunoisolates (Fig. 4A). The C-terminal fragment (CTF) of calsyntenin-1, which was abundant in APP immunoisolates, was also stable during incubation. Likewise, incubation of Rab11 immunoisolates did not result in calsyntenin-1 proteolysis (Fig. 4B). In contrast, incubation of syntaxin13 immunoisolates resulted in the appearance of cleaved calsyntenin-1 ectodomain (Fig. 4C–F). Concomitantly, the amount of calsyntenin-1 CTF was reduced after incubation

Fig. 1. Calsyntenin-1/APP vesicles contain BACE1, but no ADAM10. (**A**) Schematic representation of vesicle immunoisolation. Vesicle immunoisolations were performed with antibodies against cytosolic epitopes of vesicle-associated proteins and Dynabeads coated with protein A. Captured vesicles were isolated and washed. Vesicular proteins were eluted by lysis of the captured vesicles with a mild detergent. Note that the vesicular component bearing the antigen targeted for immunoisolation is not or only partially found in the eluate, because of its strong binding to the antibody/protein A/bead complex. Its complete elution required harsher conditions, e.g. boiling of the beads in SDS. Therefore, the antigen used for vesicle immunoisolation is not shown on the Western blots of the (mild) eluates. Examples of antigen elutions under harsh condition from the beads are shown in the panels labeled "beads". (**B**) Specificity tests of anti-APP, anti-ADAM10, and anti-BACE1 antibodies, performed by the addition of ~25 µg of recombinant antigen (GST-APPcyto, GST-ADAM10cyto, BACE1[485–501]). Saturation with recombinant antigen prevented vesicle capture. (**C**) Calsyntenin-1 organelles contained BACE1, but no ADAM10 (black box). (**D**) APP and syntaxin13 immunoisolates contain a low level of active ADAM10 and abundant BACE1. Neither BACE1 nor ADAM10 were found in Rab11 immunoisolates. (**E**) Rab5 immunoisolates contain a small amount of active ADAM10 (arrowhead) and abundant BACE1 (green box). (**F**) ADAM10 immunoisolates are devoid of calsyntenin-1, but contain a small amount of full-length APP (black box). They also contain the plasma membrane marker syntaxin4 (green box) and the early-endosomal marker Rab5 (red box). (**G**) The composition of BACE1 immunoisolates is very similar to APP immunoisolates. Note that in BACE1 immunoisolates calsyntenin-1 and APP are predominantly found in full-length forms. As mentioned above, the protein used as ligand was not or only partially found in the eluate, as its elution from the beads required SDS (boxed bands). (**H**) Summary of the vesicular components characteristic for the two distinct, non-overlapping types of calsyntenin-1 vesicles. Axonally transported calsyntenin-1-dependent replenishment vesicles (Cst1-RV) contain the early-endosomal marker Rab5 and are devoid of the recycling-endosomal marker Rab11. Axonally transported calsyntenin-1-dependent recycling-endosomal vesicles (Cst1-RE) contain Rab11, but no Rab5. The rows below indicate the components of APP, ADAM10, BACE1, Rab11, and Rab5 immunoisolates that support our conclusions. V1, vesicular fraction 1; Cst1, calsyntenin-1; +, vesicle immunoisolation using the indicated antibody together with ~ 25 µg of recombinant antigen; −, vesicle immunoisolation using the indicated antibody; ctrl, control vesicle immunoisolation performed without the indicated antibody; f, full-length; ec, ectodomain; CTF, transmembrane stump; pro, pro-form; act, active form; ER, endoplasmic reticulum; G, Golgi; TGN, trans-Golgi network; SV, secretory vesicle; PM, plasma membrane; Cst1-RV, calsyntenin-1-containing early-endosomal replenishment vesicles; Cst1-RE, calsyntenin-1-containing recycling-endosomal vesicles.

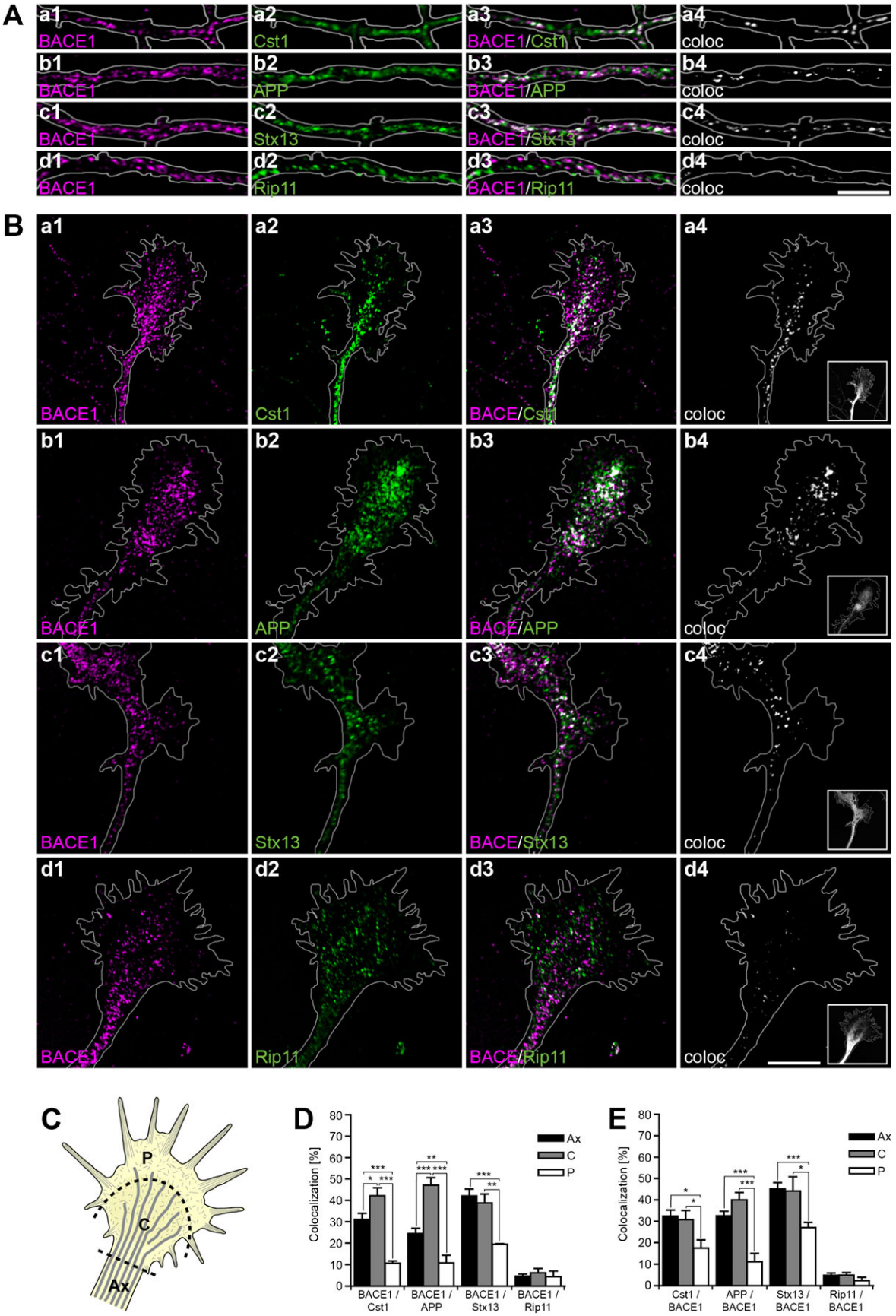

Fig. 2. See next page for legend.

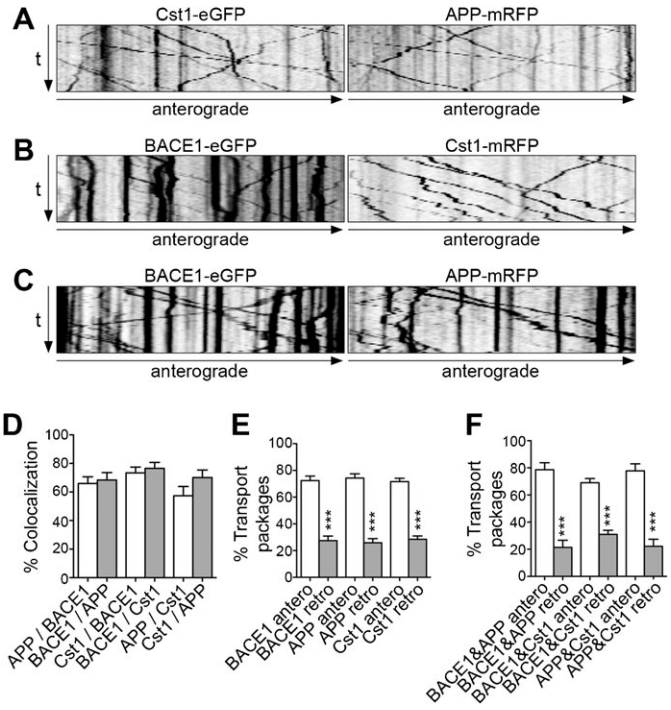

Fig. 3. Live-imaging demonstrates anterograde axonal co-transport of calsyntenin-1, APP, and BACE1. Representative kymographs of axons after co-infection of primary cultures of hippocampal neurons with adenoviral expression vectors at DIV7. (**A**) Cst1-eGFP and APP-mRFP. (**B**) BACE1-eGFP and Cst1-mRFP. (**C**) BACE1-eGFP and APP-mRFP. Note that trajectories are predominantly in anterograde direction. (**D**) Pairwise combinations demonstrate >60% colocalization of calsyntenin-1, APP, and BACE1. (**E**) Trajectories of single puncta demonstrate that BACE1, APP and Cst1 are predominantly moving anterogradely. (**F**) Over 70% of the colocalized puncta move anterogradely. Values represent mean±s.e.m. (***, $P \leq 0.001$; *t*-test; $n = 9–10$ segments).

(Fig. 4C,D,G). Blockade of calsyntenin-1 CTF degradation by DAPT indicated ongoing γ-secretase cleavage in these organelles (Fig. 4D,G). Juxtamembrane ectodomain cleavage of calsyntenin-1 and production of calsyntenin-1-CTF was prevented upon blockade of ADAM10 activity by the cell-permeable Zn^{2+}-chelator TPEN. In contrast, the selective β-secretase inhibitor IV did not prevent ectodomain cleavage of calsyntenin-1 and the production of calsyntenin-1-CTF (Fig. 4C,E). Together, these results are consistent with recent reports demonstrating calsyntenin-1 cleavage by ADAM10/17, but not by BACE1 (Hata et al., 2009).

Based on our previous characterizations, we assumed that APP immunoisolates contained predominantly components of early-endosomal calsyntenin-1 vesicles that were on anterograde axonal transport. Rab11 immunoisolates reflected the recycling-endosomal fraction of calsyntenin-1 vesicles, which was devoid of APP, while syntaxin13 immunoisolates reflected the sum of endosomal vesicles. Therefore, our results imply that calsyntenin-1 is proteolytically degraded in EEs.

Evidence for protection of APP from BACE1 during anterograde axonal co-transport in calsyntenin-1 organelles

In contrast to calsyntenin-1, the full-length forms of APP remained unaltered during incubation of syntaxin13 vesicles (Fig. 4C,D,H–K). To understand the band pattern found in the various vesicle immunoisolations we also analyzed the maturational glycosylation pattern by cleaving glycoproteins of the V1 fraction and syntaxin13 immunoisolates with PNGaseF and EndoH (Fig. 4L). The single major band of calsyntenin-1 responded to PNGaseF with a clear down-shift, while EndoH did not induce a change, indicating that calsyntenin-1 was exclusively represented by its mature, fully glycosylated form in these samples. Likewise, all three major bands of APP responded to PNGaseF with a down-shift. EndoH, in contrast, left the upper two bands of APP unchanged, but induced a down-shift of the lowest band. In all samples, we found no differences in the band patterns tested with antibodies against N- and C-terminally located epitopes of APP. In accordance with previous analyses of brain tissue samples (Buxbaum et al., 1998) and of cell lysates from cultured cortical neurons (Hoey et al., 2009), we concluded that the two upper high-molecular mass bands of APP identified in the V1 membrane input and in syntaxin13 immunoisolates (Fig. 4C,D) correspond to glycosylation variants of mature full-length APP, while the lower band represents immature full-length APP carrying high-mannose carbohydrate chains. APP in these samples was not cleaved, as the band patterns obtained with antibodies against the N- and the C-terminus of APP were identical. Because the band pattern of APP in syntaxin13 immunoisolates did not change upon vesicle incubation, we concluded that the bulk of APP is stable in syntaxin13-positive endosomal compartments, including EEs, fast recycling endosomes, as well as the calsyntenin-1-dependent anterograde axonal carriers. The fact that the APP fraction that is degraded in EEs during its peripheral recycling pathway was not detected in syntaxin13 immunoisolates indicates that APP of the calsyntenin-1/APP trafficking route vastly predominates over the amount of APP contained in the other APP-containing vesicles, including early-endosomal APP.

In accordance with the notion of a calsyntenin-1-dependent, protected route for anterograde axonal transport of APP, calsyntenin-1 immunoisolates contained predominantly full-length APP and their incubation did not result in APP processing (Fig. 4M). This is in striking contrast to early-endosomal Rab5 and Rab4 immunoisolates in which cleaved APP was predominant (Steuble et al., 2010). Taken together, these results indicate that APP is not cleaved along its anterograde transport in which it is accompanied by calsyntenin-1. Degradation of APP takes place upon arrival in EEs of growth cones and proteolytic degradation of calsyntenin-1.

Fig. 2. Calsyntenin-1/APP/BACE1 transport packages are found along axons and in growth cones. Immunofluorescence staining of dissociated hippocampal neurons. Black-and-white masks (a4–d4) were generated to emphasize the colocalization in axons (**A**) and growth cones (**B**). Inserts (a4–d4) show stainings of the axonal marker Tau-1. Note that BACE1 (a1–d1) colocalizes with calsyntenin-1 (a2,a3), APP (b2,b3), and Stx13 (c2,c3), but not with Rip11 (d2,d3). (**C**) Schematic representation of the C- and P-region of the growth cone. (**D**) Fractions of BACE1 puncta that are colocalized with calsyntenin-1, APP, syntaxin13, and Rip11 puncta. Note that BACE1 colocalizes with calsyntenin-1, APP, and syntaxin13 along axons and in the C-domain of growth cones. (**E**) Fractions of calsyntenin-1, APP, syntaxin13, and Rip11 puncta that are colocalized with BACE1 puncta. Note that the colocalization with BACE1 is confined to axons and the C-domain of growth cones. Values represent mean±s.e.m. (*, $P \leq 0.05$; **, $P \leq 0.005$; ***, $P \leq 0.001$; *t*-test; $n = 4$ growth cones; $n = 8$ axons). Ax, axon; C, C-domain of growth cone; P, P-domain of growth cone. Scale bars, 5 µm in Ad4, 10 µm in Bd4.

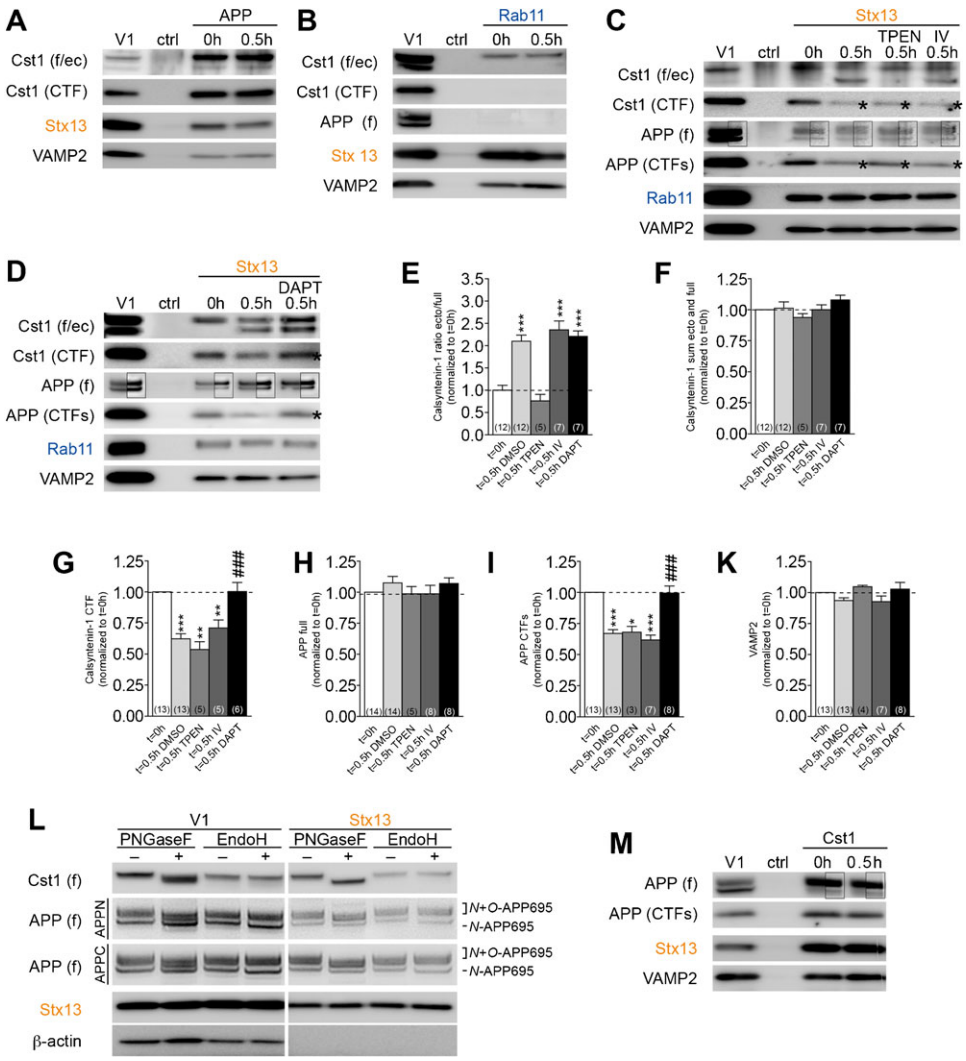

Fig. 4. Calsyntenin-1 is cleaved by ADAM10 in early endosomes. Immunoisolated organelles were solubilized immediately or after incubation for 30 minutes at 37℃ without or with inhibitors. Full-length calsyntenin-1 and APP, as well as their cleavage products, were assessed by Western blotting. The endosomal markers Rab11, syntaxin13, and VAMP2 were used as loading controls. (**A**,**B**) Calsyntenin-1 is not cleaved in APP and Rab11 organelles. (**C**) Calsyntenin-1 cleavage in syntaxin13 organelles is prevented by 20 µM ADAM10 inhibitor TPEN, but not by 10 µM BACE1 inhibitor IV. Note the decrease of the CTFs of both calsyntenin-1 and APP after incubation (asterisks). (**D**) Addition of 2 µM γ-secretase inhibitor DAPT prevented the decrease of calsyntenin-1 and APP CTFs (asterisks). (**E**–**K**) Densitometric quantification of calsyntenin-1 and APP cleavage in syntaxin13 organelles. (E) Ratios of calyntenin-1 ectodomain versus full-length. (F) Sums of calsyntenin-1 ectodomain and full-length bands demonstrate equal gel loading. (G) Degradation of calsyntenin-1 CTF during incubation is prevented by DAPT. (H) Full-length APP is stable. (I) APP CTFs are decreased after incubation, their degradation is blocked by DAPT. (K) VAMP2 levels remain unaltered throughout the incubation experiments. Number of measurements obtained in at least three independent experiments are given within the bars; *, $P<0.05$; **, $P<0.005$; ***, $P<0.001$, paired *t*-test relative to t=0 h; ###, $P<0.001$, paired *t*-test relative to t=0.5 h DMSO. (**L**) Deglycosylation of V1 membranes (left panel) and syntaxin13 organelles (right panel) with PNGaseF and endoglycosidase H. The N-terminal (APPN) and the C-terminal (APPC) antibodies detected identical band patterns in all samples. No cleaved ectodomain of APP can be detected. (**M**) APP is not degraded in calsyntenin-1 vesicles. V1, vesicular fraction 1; ctrl, control vesicle immunoisolation performed without the indicated antibody; f, full-length; ec, ectodomain; CTF, transmembrane stump; TPEN, an inhibitor of Zn^{2+}-dependent matrix metalloproteases; IV, β-secretase inhibitor IV; DAPT, γ-secretase inhibitor DAPT; DMSO, dimethyl sulfoxide; APPN, antibody against N-terminal epitope(s) of APP; APPC, antibody against C-terminal epitope(s) of APP; N+O-APP695, N- + O-glycosylated mature form of APP695; N-APP695, high-mannose N-glycosylated immature form of APP695.

Down-regulation of calsyntenin-1 results in premature encounter of APP and ADAM10

Because ADAM10 was excluded from calsyntenin-1/APP vesicles, we assumed that APP and ADAM10 did not encounter each other until both had reached the plasma membrane via distinct pathways. We tested whether reduced calsyntenin-1 levels resulted in altered APP trafficking and premature contact of APP with ADAM10. To this end we down-regulated calsyntenin-1 in hippocampal neurons by RNAi and performed immunocytochemical double-staining for ADAM10 and APP (Fig. 5). The specificity of anti-calsyntenin-1, anti-APP, and anti-ADAM10 antibodies was demonstrated by the absence of an immunofluorescence signal after pre-incubation of the antibody with the corresponding antigen (supplementary material Fig. S2). Down-regulation of calsyntenin-1 by RNAi was measured in confocal images of cultured cortical neurons (Fig. 6A,B) and by

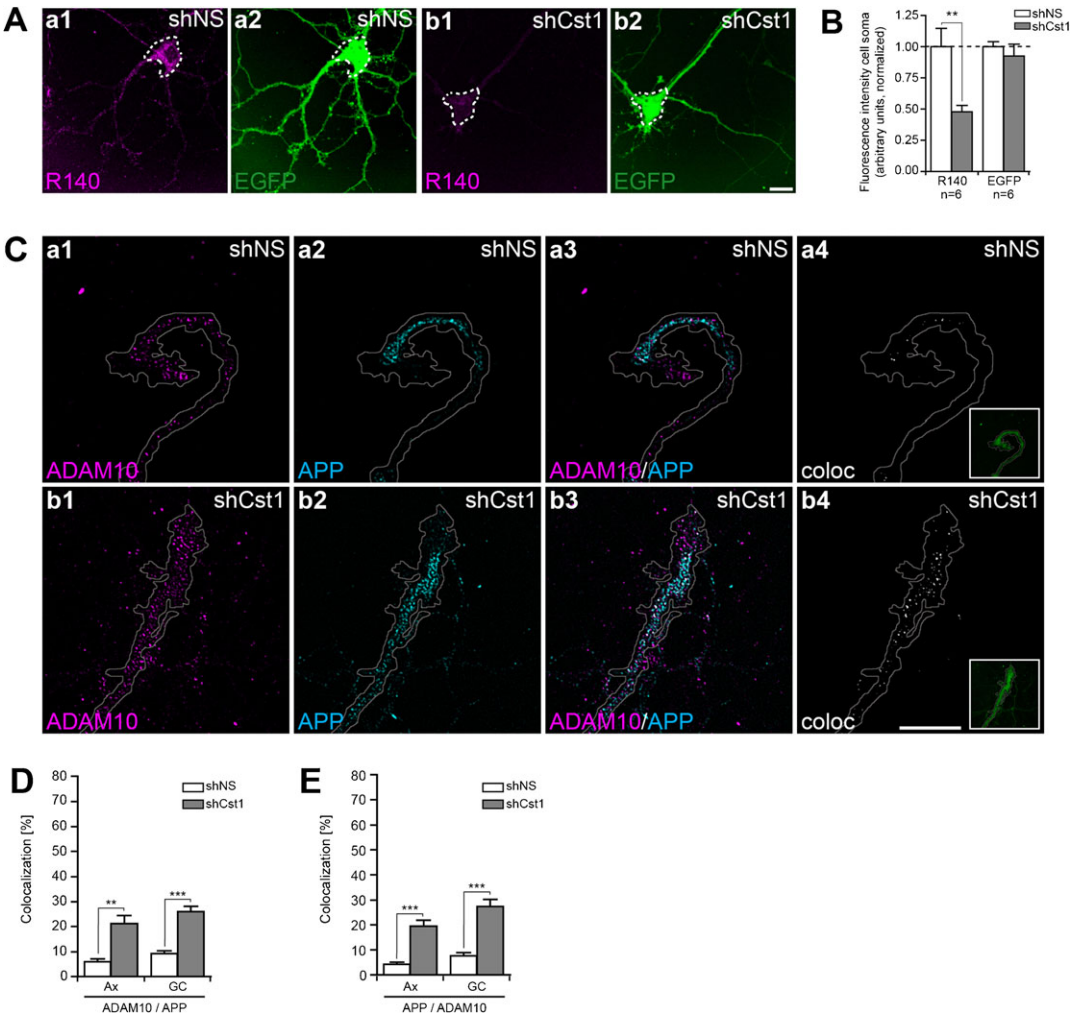

Fig. 5. Downregulation of calsyntenin-1 by RNAi results in axonal cotransport of APP and ADAM10. Hippocampal neurons were infected with rAAVs (shNS, shCst1) and immunostained after 10 DIV. (**A**) Double-staining for calsyntenin-1 (a1,b1) and eGFP (a2,b2) of a representative neuron expressing shNS::eGFP (a) and a neuron expressing shCst1::eGFP (b). (**B**) Relative fluorescence intensities of cell somas (dotted lines in A). Values indicate mean±s.e.m. (**$P \leq 0.005$; *t*-test; $n=2$, with $n=3$ each). (**C**) Confocal microscopic images of growth cones after immunocytochemical staining of ADAM10 and APP. Black-and-white masks (a4,b4) were generated to emphasize the colocalization. Inserts (a4,b4) display eGFP expression. Note that colocalization of ADAM10 (a1,b1) with APP (a2,b2) is increased when calsyntenin-1 is down-regulated (b1–b4). (**D**) Fraction of ADAM10 puncta which are colocalized with APP puncta. (**E**) Fraction of APP puncta which are colocalized with ADAM10 puncta. Values represent mean±s.e.m. (*, $P \leq 0.05$; ***, $P \leq 0.001$; *t*-test; $n=4$, with $n=2$–4 growth cones and axons each, total $n=13$ each). Scale bars, 10 µm in Ab2 and Cb4. shNS, RNAi with a short-hairpin RNA construct containing a nonsense sequence; shCst1, RNAi with a short-hairpin RNA construct containing a calsyntenin-1-derived sequence; R140, anti-calsyntenin-1 antibody 140, EGFP, anti-EGFP antibody; Ax, axon; GC, growth cone.

quantification of the band intensities in Western blots (Fig. 6A). Down-regulation of calsyntenin-1 by 52% (Fig. 5A,B) substantially increased the colocalization of APP and ADAM10 both in axons and growth cones (Fig. 5C). Calsyntenin-1-specific shRNA increased the fraction of ADAM10 vesicles containing APP from 6% to 21% in axons and from 9% to 26% in growth cones, compared to treatment with nonsense shRNA (Fig. 5D). Conversely, the fraction of APP vesicles containing ADAM10 increased from 4% to 19% in axons and from 8% to 27% in growth cones in the presence of calsyntenin-1-specific shRNA (Fig. 5E). These results suggest that the reduction of the transport capacity for APP in the sheltered calsyntenin-1/APP pathway results in mis-sorting of APP in the TGN and ectopic TGN exit with other post-Golgi carriers. Mis-sorting leads to premature exposure of APP to ADAM10.

Abrogation of anterograde axonal calsyntenin/APP transport enhances both α- and β-cleavage of APP and results in increased Aβ release

We next examined whether mis-sorting of APP into ADAM10-containing carriers affected its proteolytic processing. Upon down-regulation of calsyntenin-1 by RNAi, APP cleavage at both the α- and the β-site was enhanced (Fig. 6A,B). The normalized α-C99/β-C83 ratio after calsyntenin-1 RNAi was 1.05 and did not significantly differ from the α-C99/β-C83 ratio found in the nonsense controls. Because a proportionally equal increase of both C-terminal fragments could result either from equally enhanced cleavage at the α- and β-site or reduced γ-cleavage, we also determined Aβ after RNAi down-regulation of calsyntenin-1. Because it has been reported that a substantial proportion of the intracellular Aβ pool is released into the extracellular space

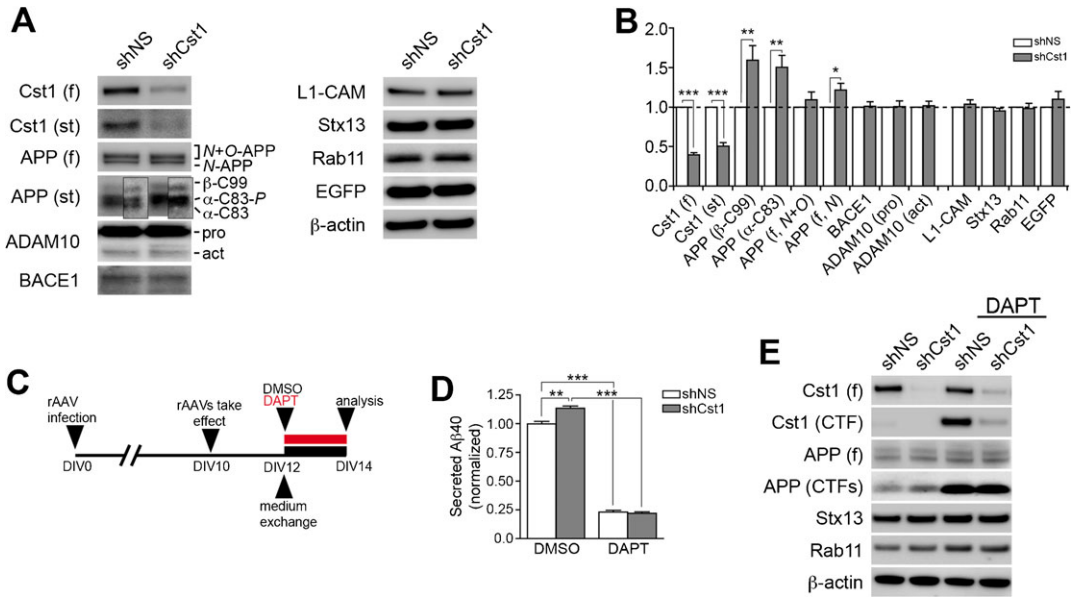

Fig. 6. Downregulation of calsyntenin-1 by RNAi results in enhanced APP processing and increased secretion of Aβ. Cortical neurons were infected with rAAVs expressing a hairpin targeting calsyntenin-1 (shCst1) or a nonsense hairpin (shNS), together with eGFP. (**A**) Western blot of cell lysates. The signal indicated equal expression of the recombinant proteins. (**B**) Quantification of Western blots. Values indicate mean±s.e.m. (*, $P \leq 0.05$, **, $P \leq 0.005$, ***, $P \leq 0.001$; paired *t*-test; $n=3$, with $n=4$ each). (**C–E**) Measurement of Aβ secretion. (C) Cortical neurons were infected with rAAV-shCst1 or rAAV-shNS. At DIV12 new medium with DAPT (2 µM) or DMSO carrier was added. Analysis was at DIV14. (D) ELISA of secreted Aβ (1–40) from four experiments. Values indicate mean±s.e.m.. $n=14$ (DMSO) and $n=13$ (DAPT); **, $P \leq 0.005$; ***, $P \leq 0.001$, paired *t*-test. (E) Immunoblot showing the CTFs of calsyntenin-1 and APP at DIV14. Syntaxin13, Rab11, and β-actin served as loading controls. f, full-length; st, transmembrane stump; β-C99, C-terminal transmembrane stump after β-secretase cleavage; α-C83, C-terminal transmembrane stump after α-secretase cleavage; N+O-APP695, N- + O-glycosylated mature form of APP695; N-APP695, high-mannose N-glycosylated immature form of APP695; rAAV, recombinant adeno-associated virus containing an expression cassette of the shRNA construct; DAPT, γ-secretase inhibitor DAPT; DMSO, dimethyl sulfoxide.

(Haass and Selkoe, 2007), we quantified Aβ levels in neuronal culture medium after down-regulation of calsyntenin-1, using ELISA (Fig. 6C–E). Compared to control cultures, Aβ secretion was significantly increased by 13% from 260±16 pg/ml to 296±21 pg/ml, $P \leq 0.005$ (Fig. 6D). To test whether the detected Aβ (1–40) was attributable to release from live neurons we compared release in the absence and presence of the γ-secretase inhibitor DAPT. DAPT reduced the amount of released Aβ by 77%, $P \leq 0.001$ (Fig. 6D) and resulted in the accumulation of calsyntenin-1 and APP CTFs (Fig. 6E). The increase of Aβ argued against inhibition of γ-secretase as a consequence of calsyntenin-1 down-regulation. Protein levels of ADAM10, BACE1, L1-CAM, syntaxin13, Rab11, and β-actin were identical throughout experimental treatments. We concluded that calsyntenin-1 protects APP from proteolytic processing by its α- and β-secretases during axonal transport.

Discussion

Immunoisolated trafficking organelles comprise a combination of multiple vesicular subpopulations – a methodological note

Trafficking organelles are elements of a highly dynamic system of numerous complex and interconnected pathways. The contacts, fusions, and scissions of distinct organelles result in the exchange of "organelle-specific" components. To maintain the proper composition of organelles, components "lost in action" are returned to the location of their function by recycling pathways (Maxfield and McGraw, 2004). This explains why most, if not all of the well characterized "vesicular marker proteins" are also found at lower concentrations in vesicles fusing to or leaving from the respective organelle, as well as in vesicles serving as recycling pathways to maintain the specific molecular inventory of the respective vesicle.

Vesicular cargo proteins are shipped along their intracellular path from one organelle to the other. Therefore, vesicle immunoisolations based on cargo proteins represent a mixture of organelles that are visited by the cargo protein along its trajectory. Also, when vesicles are isolated based on a bona fide "specific" structural or functional component of a trafficking organelle, such as syntaxin13 or Rab5, a clean population of the respective organelle cannot be expected.

Attributable to the composite nature of most immunoisolates, the detection of a given protein by mass spectrometry or Western blotting does not allow for its unequivocal localization. To overcome this drawback, we generated immunoisolates based on partially overlapping vesicular markers. This approach allowed us to more specifically assign the localization of a protein, based on its presence or absence in two or more partially overlapping populations.

The axonal calsytenin-1/APP (Rab11-negative) vesicles represent an anterograde axonal route for delivery of APP and BACE1 to the rapid (early-endosomal) APP recycling pathway of the growth cone

Live-imaging demonstrated that calsyntenin-1-containing organelles move in anterograde direction along axons, based on a specific interaction of calsyntenin-1 with Kinesin-1 (Konecna et al., 2006; Araki et al., 2007). Subsequent proteomic and immunocytochemical characterizations revealed that the early-endosomal fraction of calsyntenin-1 organelles contains APP

(Steuble et al., 2010). In extension of these studies, we showed here that BACE1 colocalized with calsyntenin-1, APP, and syntaxin13 along axons and in growth cones. We propose that calsyntenin-1, APP, and BACE1 are sorted at the TGN for common *post*-Golgi anterograde transport. This view is supported by our previous data in COS7 cells, in which calsyntenin-1 and APP intimately colocalized in the TGN and left the TGN together via the formation of tubular structures (Ludwig et al., 2009).

Large pleiomorphic structures in the C-region of growth cones represent the distal end point of the axonal calsyntenin-1/APP trajectory (Steuble et al., 2010). In accordance, live organelle tracking revealed the fusion between calsyntenin-1/APP-tubular structures emerging from the TGN and syntaxin13-labeled structures with early-endosomal morphology (Ludwig et al., 2009). Together, these results strongly suggest that the combined anterograde axonal transportation of APP and BACE1 in calsyntenin-1/Kinesin-1-powered vesicles ends in sorting endosomes of the C-region of the growth cone. Such sorting endosomes have been characterized as a major hub for the peripheral recycling of adhesive and growth-promoting cell surface proteins of the growth cone (Kamiguchi and Lemmon, 2000; Kamiguchi, 2003).

Calsyntenin-1/APP organelles shelter APP during anterograde axonal transport from contact with ADAM10 and protect it from co-transported BACE1

Both organelle immunoisolation and immunocytochemistry characterized the calsyntenin-1/APP vesicle as a carrier in which APP is sheltered from ADAM10. We previously found that calsyntenin-1 is essential for the formation of the calsyntenin-1/APP carrier in the TGN and speculated that the absence of calsyntenin-1 may result in leakage of APP into other anterograde carriers (Ludwig et al., 2009). Here, we show that down-regulation of calsyntenin-1 indeed abolishes the separate anterograde trafficking of APP and ADAM10 along axons. Thus, a reduced capacity of the calsyntenin-1/APP route results in premature encounter of APP and ADAM10, which in turn provides a plausible explanation for the increased α-cleavage found as a result of RNAi-mediated down-regulation of calsyntenin-1.

We also found that a substantial proportion of BACE1 destined for EEs of the growth cone is transported along axons together with APP. Our results are in accordance with a study indicating a common Kinesin-mediated transport compartment for BACE and APP in axons of the sciatic nerve, the dorsal root ganglia, and the corpus callosum (Kamal et al., 2001). In contrast, a study in axons of retinal ganglion cells indicated separate transport of YFP-APP and CFP-BACE1 (Goldsbury et al., 2006). Possible explanations for such apparently conflicting observations include differences in the molecular cargo of the distinct trafficking organelles in different neuronal populations, as well as experimentally induced alterations in the molecular cargo due to overexpression of tagged proteins.

The colocalization of BACE1 and APP during calsyntenin-1-mediated axonal transport suggested that β-cleavage of APP may occur before it reaches the growth cone. However, several studies identified the early endosome as the major site of β-cleavage of APP that was imported via endocytosis from the plasma membrane (Koo and Squazzo, 1994; Perez et al., 1999; Kinoshita et al., 2003; Rajendran et al., 2006; Rajendran et al., 2008; He et al., 2007). Consistent with this concept, we found predominantly full-length APP in calsyntenin-1, APP, and BACE1 immunoisolates, indicating that APP is not or only slowly processed during axonal transport. This implies the existence of a mechanism that protects APP from proteolysis en route to the growth cone. Several pieces of circumstantial evidence point to calsyntenin-1 as an essential protective agent. Firstly, calsyntenin-1 and APP co-localize from TGN exit to the early endosomal sorting compartment in the C-domain of the growth cone. Secondly, the EE, the major site of APP cleavage by BACE1, coincides with the endpoint of calsyntenin-1/APP colocalization through proteolytic cleavage of calsyntenin-1. Thirdly, knock-down of calsyntenin-1 via RNAi markedly increased the relative amounts of β-CTFs of APP and the secretion of Aβ. Fourthly, APP cleavage in the EE was reported to depend on its ongoing endocytosis from the plasma membrane (Perez et al., 1999; Carey et al., 2005; Cirrito et al., 2008), indicating that endocytosed APP is preferred over anterogradely delivered APP for BACE1 cleavage in EEs.

The mechanism that keeps BACE1 away from APP or that inhibits its activity during its calsyntenin-1/Kinesin-1-mediated anterograde transport is open to conjecture. A mechanism controlling BACE1 activity via redistribution between lipid domains could involve the X11/Mint proteins. The interaction of X11/Mint proteins with APP was found to slow down cellular APP processing (Borg et al., 1998). The formation of a tripartite complex of X11β/Mint2 bound directly to the cytoplasmic segments of calsyntenin-1 and APP was subsequently shown to retard APP processing (Araki et al., 2003).

The reticulon family, in particular reticulon-3 and reticulon-4/Nogo, may directly inactivate BACE1 (He et al., 2004; Murayama et al., 2006). Similarly, complex formation with CSS, the copper chaperone for superoxide dismutase, could inactivate BACE1 (Angeletti et al., 2005). Recent reports indicate an interaction between X11/Mint proteins and CSS (McLoughlin et al., 2001). Based on these observations, it has been suggested that BACE1 could be connected to the APP/X11-complex via CSS and that the formation of a neuronal APP/X11/CSS/BACE1 complex could have an inhibitory effect on BACE1 (Miller et al., 2006). Combining these views, it is tempting to speculate that calsyntenin-1 may interact with the APP/X11/CSS/BACE1 complex in a way that enhances its inhibitory effect on BACE1.

Our analyses identified several components of these BACE1-inactivating mechanisms in calsyntenin-1 vesicles. We identified reticulon-4/Nogo by mass spectrometry and X11β/Mint2 by Western blotting (Steuble et al., 2010). Therefore, it is plausible that the BACE1-inhibiting effect of these compartments maintains APP in full-length form during its calsyntenin-1-mediated anterograde axonal trajectory.

Cleavage of calsyntenin-1 by endocytosed ADAM10 may terminate the protection of APP and release axonally transported APP into the peripheral cycling pathway

Our studies which aimed at cell-surface biotinylation of calsyntenin-1 failed despite numerous attempts (not shown), thus suggesting that calsyntenin-1 was proteolytically processed in an internal compartment or within a very short time after its arrival at the plasma membrane. Similarly, the striking clearance of calsyntenin-1 from APP vesicles at the transition from the C- to the P-domain of growth cones suggested an internal compartment as a major site of calsyntenin-1 proteolysis (Steuble et al., 2010). Based on these and the results of our

vesicle incubation studies demonstrating that calsyntenin-1 is cleaved in syntaxin13 immunoisolates, but not in Rab11 and APP immunoisolates, we concluded that calsyntenin-1 is cleaved in early endosomes. Accordingly, most cleaved calsyntenin-1 was found in Rab5 immunoisolates.

A recent report indicated that both ADAM10 and ADAM17, but not BACE1, are capable of cleaving calsyntenin-1 (Hata et al., 2009). Because ADAM17 was reported to be expressed in astrocytes and endothelial cells, but not in neurons (Goddard et al., 2001), we suspected ADAM10 to be the principle terminator of the calsyntenin-1-mediated protection of APP along anterograde axonal transport. We found a relatively strong immunoreactivity for active ADAM10 in Rab5 immunoisolates indicating that some ADAM10 may be endocytosed from the plasma membrane into EEs. In addition, active ADAM10 was found in syntaxin13 and APP, but not in Rab11 or calsyntenin-1 immunoisolates. Contamination with plasma membrane components as a trivial explanation for the detection of ADAM10 in these immunoisolates could be excluded based on the absence of syntaxin4. Because the major fraction of ADAM10 is thought to reside on the plasma membrane and because calsyntenin-1 vesicles do not contain ADAM10, we conclude that endocytosis from the plasma membrane is the major origin of early-endosomal ADAM10. This conclusion is supported by a recent demonstration of enhanced surface expression of ADAM10 after inhibition of endocytosis (Carey et al., 2011).

Indeed, ADAM10, but not BACE1, is capable of ectodomain cleavage of calsyntenin-1 (Hata et al., 2009). Selective cleavage of calsyntenin-1 in EEs could disassemble the calsyntenin-1-dependent APP-protecting complex and release APP, which in turn could join the bulk of APP cycling between the plasma membrane and EEs of the growth cone. Such a de-protection mechanism is conceivable under the assumption that calsyntenin-1 is more sensitive to juxtamembrane cleavage by ADAM10 than APP. Indeed, there is evidence for such a scenario. Most calsyntenin-1 reaching the plasma membrane via the calsyntenin-1/Rab11 route seems to be rapidly cleaved, as we could not detect any full-length calsyntenin-1 at the plasma membrane. In contrast, only a fraction of full-length APP reaching the plasma membrane is cleaved by ADAM10, while the rest is endocytosed and enters the peripheral APP recycling pathway (Haass et al., 1992; Koo et al., 1996; Yamazaki et al., 1996; Marquez-Sterling et al., 1997; Groemer et al., 2011). Thus, full-length APP in EEs originates from two sources: from anterograde delivery via calsyntenin-1-mediated axonal transport, and from endocytosis. Previous reports indeed support the notion that APP cleavage in EEs may affect a fraction of both endocytosed and anterogradely transported APP. Based on the observation that blockade of endocytosis reduced the secretion of Aβ by ~ 70%, it was concluded that primarily endocytosed APP was cleaved (Cirrito et al., 2008). In contrast, evidence for APP cleavage without prior surface exposure was provided in a study where exocytosis was blocked (Khvotchev and Südhof, 2004).

Altogether, our studies clearly characterize calsyntenin-1 as a one-way protein. Its functional journey starts when it orchestrates the formation of a vesicular or tubulovesicular structure at the TGN to recruit Kinesin-1, APP and BACE1 for plus-end-directed transport along microtubules (Ludwig et al., 2009). The journey ends with its proteolytic degradation upon arrival at the endosome of the growth cone (Fig. 7).

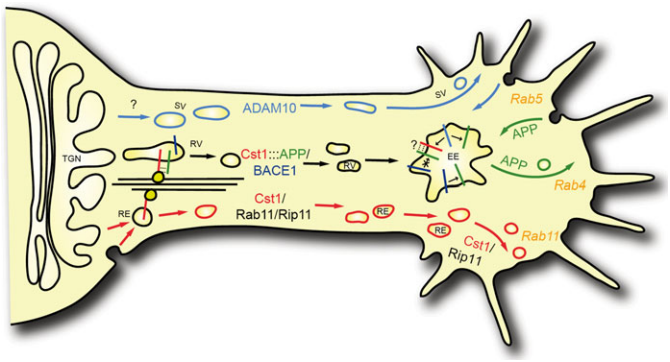

Fig. 7. Model of the itinerary of vesicular calsyntenin-1/APP for anterograde axonal transport to the growth cone. Calsyntenin-1/APP/BACE1 transport packages (black) deliver full-length APP to EEs in the C-domain of growth cones, thus replenishing full-length APP lost in the rapid recycling endosomal pathway of the growth cone by proteolysis. Calsyntenin-1/Rab11/Rip11 transport packages (red) provide an independent APP-free anterograde transport route, possibly corresponding to the anterograde axonal leg of the long recycling pathway (Lasiecka and Winckler, 2011). ADAM10 is transported on a calsyntenin-1-independent transport route. TGN, trans-Golgi network; SV, secretory vesicle; RV, calsyntenin-1-containing early-endosomal replenishment vesicle; RE, calsyntenin-1-containing recycling-endosomal vesicle; EE, early endosome.

Materials and Methods

Antibodies and reagents

Polyclonal rabbit anti-calsyntenin antibodies R85 and R140 have been described earlier (Konecna et al., 2006; Steuble et al., 2010). Anti-Rip11 was provided by Mitsuo Tagaya (Tokyo University of Pharmacy and Life Science) and anti-L1-CAM was provided by Vance Lemmon (University of Miami). Anti-nicastrin (Ab3444) was from Abcam, Cambridgeshire, UK. Anti-GM130 (610822), anti-Mint2 (76120), anti-Rab11 (6100656), anti-Rab4 (610888), anti-syntaxin4 (610439), and anti-syntaxin6 (610635) were from BD Biosciences, Allschwil, Switzerland. Anti-ADAM10 (422751) was from Calbiochem, Läufelfingen, Switzerland. Anti-APP (MAB348), anti-PS1 (MAB5232), and anti-Tau-1 (MAB3420) were from Chemicon, Lucerne, Switzerland. Anti-Rab11 (71-5300) was from Invitrogen, Basel, Switzerland. Anti-GFP (1181446001) was from Roche, Basel, Switzerland. Anti-Pen-2 (36-7200), anti-Grp78 (Sc-1050), anti-Mint2 (Sc-30135), anti-PS1 (Sc-7860), anti-Rab5a (Sc-309), and anti-Rab5 (Sc-46692) were from Santa Cruz Biotechnology, Nunningen, Switzerland. Anti-ADAM10 (A2726), anti-APP (A8717) and anti-β-actin (A5316) were from Sigma-Aldrich, Buchs, Switzerland. Anti-syntaxin13 (110132), anti-syntaxin16 (110162), anti-VAMP2 (104211), anti-VAMP4 (136002), and anti-Vti1a (165002) were from Synaptic Systems, Göttingen, Germany. Anti-BACE1 (PA1-757) was from Thermo Scientific, Wohlen, Switzerland. Fluorescent secondary antibodies (Cy3-, FITC-, Cy5-, and DyLight649-conjugated) were from Jackson ImmunoResearch Laboratories, West Grove, PA, USA and used at 2.5 µg/ml.

The γ-secretase inhibitor DAPT (1 mM in DMSO) and TPEN, a cell-permeable inhibitor of Zn^{2+}-dependent matrix metalloproteases (10 mM in DMSO) were purchased from Sigma-Aldrich. The β-secretase inhibitor IV (20 mM in DMSO) was purchased from Calbiochem. N-glycosidase F and endoglycosidase H were from Roche.

Subcellular fractionation of mouse brain and immunoisolation of vesicular organelles

The V1 membrane fraction was prepared from P7 mouse brains by differential centrifugation as previously described (Morfini et al., 2002; Konecna et al., 2006; Steuble et al., 2010). Washed V1 pellets were resuspended in IP buffer (PBS, 320 mM sucrose, 5 mM EDTA, pH 7.4) and stirred for 1 h at 4℃. For immunoblotting, 2 mg magnetic Dynabeads M-280 protein A (Invitrogen) were incubated with 10 µg IgG for 40 min and washed four times in IP buffer. V1 inputs were adjusted to ~0.7 mg/ml with IP buffer and incubated with pre-coated beads for 1 h at 4℃. Beads with immunoisolated organelles were washed 10 times with 1 ml IP buffer, once with 20 mM Tris·Cl, pH 7.4, and subsequently incubated in 50 µl 20 mM Tris·Cl, pH 7.4, 0.1% (v/v) Triton X-100 for 30 min at 25℃.

For Western blotting, 20 µg protein from input and 40 µl eluate were resolved on 4–12% NuPage Bis-Tris gels (Invitrogen). Bead contents were analyzed separately. Immunoblots were imaged with a Fuji LAS-3000 Lite CCD camera (Raytest AG, Wetzikon, Switzerland) and quantified using the AIDA 2D multi labeling software (version 3.4; Raytest AG).

For *in vitro* incubation experiments, immunoisolated organelles were incubated for 30 min at 37℃ in PBS, pH 7.4, 2 mM $MgCl_2$, 3 mM ATP, supplemented with vehicle or 2 µM DAPT, 20 µM TPEN, and 10 µM β-secretase inhibitor IV, respectively (Yamashiro et al., 1983).

Cultures of dissociated hippocampal and cortical neurons

For immunocytochemistry, 5,000 dissociated hippocampal cells/cm^2 from E19 NMRI mice were plated onto poly-L-lysine-coated (Sigma-Aldrich) glass coverslips and co-cultured face-to-face with a monolayer of astrocytes (Banker, 1980). For Western blotting, 500,000 dissociated cortical cells/cm^2 were plated onto poly-L-lysine-coated 12-well plates. Cells were grown in neurobasal medium supplemented with B27, 5 mM glutamine, and antibiotics (penicillin/streptomycin).

Immunocytochemistry

For immunofluorescence analysis, neurons were fixed in 4% paraformaldehyde, 4% sucrose in PBS, pH 7.4, for 10 min at room temperature. Samples were blocked for 1 h in 10% fetal calf serum, 0.1% saponin in PBS, pH 7.4. Neurons were then exposed to primary antibodies in 3% fetal calf serum, 0.1% saponin in PBS, pH 7.4, overnight at 4℃, then incubated for 1 h with Cy3-, FITC-, Cy5-, or DyLight649-conjugated secondary antibodies and mounted in Vectashield medium (Vector Laboratories, Burlingame, CA, USA).

In some experiments, double-labeling had to be carried out with two primary antibodies raised in the same species. In this case, neurons were first labeled with the first primary antibody, washed, and incubated with an excess of goat anti-rabbit Fab fragments (1:10) following the manufacturer's instructions (Jackson ImmunoResearch Laboratories). After extensive washing, cells were incubated with the second primary antibody, followed by incubation with anti-goat and anti-rabbit secondary antibodies. Two control experiments confirmed the specificity of this approach. Firstly, it was shown that FITC-conjugated anti-rabbit secondary antibody was not immunoreactive in the presence of primary rabbit antibody masked with goat Fab fragments. This control served to stringently define the confocal settings during imaging and image processing. Secondly, the staining patterns of double-labeled cells were shown to be identical to immunostainings of the respective antibodies alone.

Confocal images were taken with a Leica confocal laser scanning microscope TCS-SP2 at a resolution of 1024×1024 pixels using a Leica PL Apo 63× (NA=1.32) objective (Leica, Heerbrugg, Switzerland). Colocalization was analyzed by ImageJ (version 1.38×; National Institutes of Health, Betheseda, MA, USA). Statistical analyses were performed with Prism (version 4.0; GraphPad Software Inc, La Jolla, CA, USA). RGB images were used to determine the degree of colocalization between the red, green, and blue channels using the colocalization RGB plugin of ImageJ. Puncta were counted from binarized images with the particle analyzer tool, minimum size of counted puncta set to 20 pixels. Data shown are mean±s.e.m. of at least four separate images.

Generation of recombinant adeno-associated viruses (AAV) for RNAi

To generate calsyntenin-1 small hairpin knockdown construct pBlueU6-siCst1.1, the promoter of the mouse U6 RNA gene (GenBank X06980) was amplified from genomic DNA using oligonucleotides GCGGATCCGACGCCATCTCTA and GCTCTAGAGCGTTAACAAGGCTTTTCTCCAAGG. The resulting PCR product was digested with BamHI and XbaI and cloned into pBluescript II SK (+) (Stratagene). A 19 nt sequence targeting mouse calsyntenin-1 (548–476 bp; GenBank MMU289016) separated by a 9 nt spacer and followed by its 19 nt reverse complementary sequence plus a termination signal consisting of five thymidines was cloned into pBlueU6 immediately downstream of the U6 promoter. As a control, a 19 nt sequence derived from the Oryza sativa genome (GenBank EF576615.1) was cloned into pBlueU6 to generate pBlueU6-nonsense (NS) plasmid. The small-hairpin RNA expression cassettes in pBlueU6 were subcloned into psubAAV2-CMV-eGFPN1 to generate psubAAV2-eGFP-siCst1.1 and psubAAV2-eGFP-NS. Helper virus-free recombinant adeno-associated viruses (rAAVs) were generated in HEK293T by calcium phosphate cotransfection of rAAV vector plasmid and pDG helper plasmid. Cells were collected and lysed 48 h post transfection. The rAAV particles were purified by iodixanol gradient ultracentrifugation and concentrated with a Biomax-100K nominal molecular weight limit (NMWL) filter device (Millipore UFC910024) (Grimm et al., 1998).

Dissociated hippocampal and cortical neurons were infected with equal amounts of rAAVs on the day of plating and cultivated for 10 or 14 days. Imaging and analysis was carried out by an experimenter who was blind to the kind of rAAV applied.

Generation of recombinant adenovirus

APP-mRFP, BACE-eGFP, meGFP-Cst-1, and mRFP-Cst-1 were subcloned into a transfer vector to generate infectious adenovirus H5, as previously described (Frischknecht et al., 2008). Viral particles were purified by a single centrifugation over a CsCl step gradient (1.25 and 1.4 g/ml CsCl). Expression of recombinant proteins was assessed by immunoblotting of lysates of infected HEK-293 cells.

Live-imaging of axonal transport of fluorescently-tagged calsyntenin-1, APP, and BACE1

Cultures of dissociated hippocampal neurons were co-infected with adenovirus on DIV7 and imaged after two days in a Ludin imaging chamber (Life Imaging Services, Basel, Switzerland) under constant perfusion with (in mM): 119 NaCl, 2.5 KCl, 2 $CaCl_2$, 2 $MgCl_2$, 30 glucose, and 25 HEPES, pH 7.4. Widefield images were acquired on a Leica LX microscope equipped with a 100×, 1.4 NA, oil objective, a Hamamatsu-C9100-13 EM-CCD camera system (500×500 px, Hamamatsu, Hersching am Ammersee, Germany). Images were taken at 1 sec intervals for a period of 1 min. Axons were identified according to morphological criteria (thin and at least two times longer than dendrites). Anterograde and retrograde vesicle transport was quantified independently for each channel and subsequently tested for colocalization. The quantification was performed manually and included only vesicles that were clearly traceable for at least 20 sec.

ELISA for murine Aβ

Cortical neurons were infected with the respective rAAVs on the day of plating and kept with virus for 12 DIV. Neurobasal medium was removed and neurons were washed twice with PBS, pH 7.4, to remove Aβ that had accumulated during cultivation. Then, 300 µl of fresh medium without phenol red, supplemented with B27, vehicle or 1 µM DAPT were added. After 2 days, 250 µl medium were harvested and centrifuged for 30 min at 100,000×g at 4℃. Samples (100 µl) were added to a mouse/rat Aβ (1–40) ELISA plate (code 27720; Immuno-Biological Laboratories, Minneapolis, MN, USA) and processed according to the manufacturer's instructions.

Glycosidase treatments *in vitro*

V1 membranes or syntaxin13 immunoisolates were processed with N-glycosidase F (PNGaseF, Roche) or endoglycosidase H (EndoH, Roche). For deglycosylation with PNGaseF, the reaction mixture (80 µl final volume) contained 10 µg protein and 4 mU PNGaseF in 10 mM EDTA, 1% β-mercaptoethanol (v/v), 0.1% SDS, and 2.75 mM Tris·Cl, pH 7.4. For deglycosylation with EndoH, the reaction mixture (80 µl final volume) contained equal amounts of protein and 2 mU EndoH in 1% β-mercaptoethanol (v/v), 0.25% SDS, and 10 mM sodium acetate, pH 5.2. Enzymes were added for 16 h at 37℃ after denaturation of protein samples at 95℃ for 5 min.

Acknowledgements

We are grateful to H. Büeler for providing parent AAV vectors. We are also indebted to E. T. Stoeckli for critical reading of the manuscript. This work was supported by grants of the Swiss National Science Foundation and the NCCR (National Center of Competence in Research) Neural Plasticity and Repair of the Swiss National Science Foundation.

Competing Interests

The authors declare that there are no competing interests.

References

Angeletti, B., Waldron, K. J., Freeman, K. B., Bawagan, H., Hussain, I., Miller, C. C., Lau, K. F., Tennant, M. E., Dennison, C., Robinson, N. J. et al. (2005). BACE1 cytoplasmic domain interacts with the copper chaperone for superoxide dismutase-1 and binds copper. *J. Biol. Chem.* **280**, 17930-17937.

Araki, Y., Tomita, S., Yamaguchi, H., Miyagi, N., Sumioka, A., Kirino, Y. and Suzuki, T. (2003). Novel cadherin-related membrane proteins, Alcadeins, enhance the X11-like protein-mediated stabilization of amyloid beta-protein precursor metabolism. *J. Biol. Chem.* **278**, 49448-49458.

Araki, Y., Kawano, T., Taru, H., Saito, Y., Wada, S., Miyamoto, K., Kobayashi, H., Ishikawa, H. O., Ohsugi, Y., Yamamoto, T. et al. (2007). The novel cargo Alcadein induces vesicle association of kinesin-1 motor components and activates axonal transport. *EMBO J.* **26**, 1475-1486.

Back, S., Haas, P., Tschäpe, J. A., Gruebl, T., Kirsch, J., Müller, U., Beyreuther, K. and Kins, S. (2007). beta-amyloid precursor protein can be transported independent of any sorting signal to the axonal and dendritic compartment. *J. Neurosci. Res.* **85**, 2580-2590.

Banker, G. A. (1980). Trophic interactions between astroglial cells and hippocampal neurons in culture. *Science* **209**, 809-810.

Borg, J. P., Yang, Y., De Taddéo-Borg, M., Margolis, B. and Turner, R. S. (1998). The X11alpha protein slows cellular amyloid precursor protein processing and reduces Abeta40 and Abeta42 secretion. *J. Biol. Chem.* **273**, 14761-14766.

Buxbaum, J. D., Thinakaran, G., Koliatsos, V., O'Callahan, J., Slunt, H. H., Price, D. L. and Sisodia, S. S. (1998). Alzheimer amyloid protein precursor in the rat

hippocampus: transport and processing through the perforant path. *J. Neurosci.* **18**, 9629-9637.

Carey, R. M., Balcz, B. A., Lopez-Coviella, I. and Slack, B. E. (2005). Inhibition of dynamin-dependent endocytosis increases shedding of the amyloid precursor protein ectodomain and reduces generation of amyloid beta protein. *BMC Cell Biol.* **6**, 30.

Carey, R. M., Blusztajn, J. K. and Slack, B. E. (2011). Surface expression and limited proteolysis of ADAM10 are increased by a dominant negative inhibitor of dynamin. *BMC Cell Biol.* **12**, 20.

Cirrito, J. R., Kang, J. E., Lee, J., Stewart, F. R., Verges, D. K., Silverio, L. M., Bu, G., Mennerick, S. and Holtzman, D. M. (2008). Endocytosis is required for synaptic activity-dependent release of amyloid-beta in vivo. *Neuron* **58**, 42-51.

Ferreira, A., Caceres, A. and Kosik, K. S. (1993). Intraneuronal compartments of the amyloid precursor protein. *J. Neurosci.* **13**, 3112-3123.

Frischknecht, R., Fejtova, A., Viesti, M., Stephan, A. and Sonderegger, P. (2008). Activity-induced synaptic capture and exocytosis of the neuronal serine protease neurotrypsin. *J. Neurosci.* **28**, 1568-1579.

Goddard, D. R., Bunning, R. A. and Woodroofe, M. N. (2001). Astrocyte and endothelial cell expression of ADAM 17 (TACE) in adult human CNS. *Glia* **34**, 267-271.

Goldsbury, C., Mocanu, M. M., Thies, E., Kaether, C., Haass, C., Keller, P., Biernat, J., Mandelkow, E. and Mandelkow, E. M. (2006). Inhibition of APP trafficking by tau protein does not increase the generation of amyloid-beta peptides. *Traffic* **7**, 873-888.

Grbovic, O. M., Mathews, P. M., Jiang, Y., Schmidt, S. D., Dinakar, R., Summers-Terio, N. B., Ceresa, B. P., Nixon, R. A. and Cataldo, A. M. (2003). Rab5-stimulated up-regulation of the endocytic pathway increases intracellular beta-cleaved amyloid precursor protein carboxyl-terminal fragment levels and Abeta production. *J. Biol. Chem.* **278**, 31261-31268.

Grimm, D., Kern, A., Rittner, K. and Kleinschmidt, J. A. (1998). Novel tools for production and purification of recombinant adenoassociated virus vectors. *Hum. Gene Ther.* **9**, 2745-2760.

Groemer, T. W., Thiel, C. S., Holt, M., Riedel, D., Hua, Y., Hüve, J., Wilhelm, B. G. and Klingauf, J. (2011). Amyloid precursor protein is trafficked and secreted via synaptic vesicles. *PLoS ONE* **6**, e18754.

Haass, C. and Selkoe, D. J. (2007). Soluble protein oligomers in neurodegeneration: lessons from the Alzheimer's amyloid beta-peptide. *Nat. Rev. Mol. Cell Biol.* **8**, 101-112.

Haass, C., Koo, E. H., Mellon, A., Hung, A. Y. and Selkoe, D. J. (1992). Targeting of cell-surface beta-amyloid precursor protein to lysosomes: alternative processing into amyloid-bearing fragments. *Nature* **357**, 500-503.

Hata, S., Fujishige, S., Araki, Y., Kato, N., Araseki, M., Nishimura, M., Hartmann, D., Saftig, P., Fahrenholz, F., Taniguchi, M. et al. (2009). Alcadein cleavages by amyloid β-precursor protein (APP) α- and γ-secretases generate small peptides, p3-Alcs, indicating Alzheimer disease-related γ-secretase dysfunction. *J. Biol. Chem.* **284**, 36024-36033.

He, W., Lu, Y., Qahwash, I., Hu, X. Y., Chang, A. and Yan, R. (2004). Reticulon family members modulate BACE1 activity and amyloid-beta peptide generation. *Nat. Med.* **10**, 959-965.

He, X., Cooley, K., Chung, C. H., Dashti, N. and Tang, J. (2007). Apolipoprotein receptor 2 and X11 α/β mediate apolipoprotein E-induced endocytosis of amyloid-β precursor protein and β-secretase, leading to amyloid-β production. *J. Neurosci.* **27**, 4052-4060.

Hintsch, G., Zurlinden, A., Meskenaite, V., Steuble, M., Fink-Widmer, K., Kinter, J. and Sonderegger, P. (2002). The calsyntenins–a family of postsynaptic membrane proteins with distinct neuronal expression patterns. *Mol. Cell. Neurosci.* **21**, 393-409.

Hoey, S. E., Williams, R. J. and Perkinton, M. S. (2009). Synaptic NMDA receptor activation stimulates alpha-secretase amyloid precursor protein processing and inhibits amyloid-beta production. *J. Neurosci.* **29**, 4442-4460.

Inomata, H., Nakamura, Y., Hayakawa, A., Takata, H., Suzuki, T., Miyazawa, K. and Kitamura, N. (2003). A scaffold protein JIP-1b enhances amyloid precursor protein phosphorylation by JNK and its association with kinesin light chain 1. *J. Biol. Chem.* **278**, 22946-22955.

Jorissen, E., Prox, J., Bernreuther, C., Weber, S., Schwanbeck, R., Serneels, L., Snellinx, A., Craessaerts, K., Thathiah, A., Tesseur, I. et al. (2010). The disintegrin/metalloproteinase ADAM10 is essential for the establishment of the brain cortex. *J. Neurosci.* **30**, 4833-4844.

Kaether, C., Skehel, P. and Dotti, C. G. (2000). Axonal membrane proteins are transported in distinct carriers: a two-color video microscopy study in cultured hippocampal neurons. *Mol. Biol. Cell* **11**, 1213-1224.

Kamal, A., Stokin, G. B., Yang, Z., Xia, C. H. and Goldstein, L. S. (2000). Axonal transport of amyloid precursor protein is mediated by direct binding to the kinesin light chain subunit of kinesin-I. *Neuron* **28**, 449-459.

Kamal, A., Almenar-Queralt, A., LeBlanc, J. F., Roberts, E. A. and Goldstein, L. S. (2001). Kinesin-mediated axonal transport of a membrane compartment containing beta-secretase and presenilin-1 requires APP. *Nature* **414**, 643-648.

Kamiguchi, H. (2003). The mechanism of axon growth: what we have learned from the cell adhesion molecule L1. *Mol. Neurobiol.* **28**, 219-228.

Kamiguchi, H. and Lemmon, V. (2000). Recycling of the cell adhesion molecule L1 in axonal growth cones. *J. Neurosci.* **20**, 3676-3686.

Kempf, M., Clement, A., Faissner, A., Lee, G. and Brandt, R. (1996). Tau binds to the distal axon early in development of polarity in a microtubule- and microfilament-dependent manner. *J. Neurosci.* **16**, 5583-5592.

Khvotchev, M. and Südhof, T. C. (2004). Proteolytic processing of amyloid-beta precursor protein by secretases does not require cell surface transport. *J. Biol. Chem.* **279**, 47101-47108.

Kinoshita, A., Fukumoto, H., Shah, T., Whelan, C. M., Irizarry, M. C. and Hyman, B. T. (2003). Demonstration by FRET of BACE interaction with the amyloid precursor protein at the cell surface and in early endosomes. *J. Cell Sci.* **116**, 3339-3346.

Kins, S., Lauther, N., Szodorai, A. and Beyreuther, K. (2006). Subcellular trafficking of the amyloid precursor protein gene family and its pathogenic role in Alzheimer's disease. *Neurodegener. Dis.* **3**, 218-226.

Koike, H., Tomioka, S., Sorimachi, H., Saido, T. C., Maruyama, K., Okuyama, A., Fujisawa-Sehara, A., Ohno, S., Suzuki, K. and Ishiura, S. (1999). Membrane-anchored metalloprotease MDC9 has an alpha-secretase activity responsible for processing the amyloid precursor protein. *Biochem. J.* **343**, 371-375.

Kojro, E. and Fahrenholz, F. (2005). The non-amyloidogenic pathway: structure and function of alpha-secretases. *Subcell. Biochem.* **38**, 105-127.

Konecna, A., Frischknecht, R., Kinter, J., Ludwig, A., Steuble, M., Meskenaite, V., Indermühle, M., Engel, M., Cen, C., Mateos, J. M. et al. (2006). Calsyntenin-1 docks vesicular cargo to kinesin-1. *Mol. Biol. Cell* **17**, 3651-3663.

Koo, E. H. and Squazzo, S. L. (1994). Evidence that production and release of amyloid beta-protein involves the endocytic pathway. *J. Biol. Chem.* **269**, 17386-17389.

Koo, E. H., Sisodia, S. S., Archer, D. R., Martin, L. J., Weidemann, A., Beyreuther, K., Fischer, P., Masters, C. L. and Price, D. L. (1990). Precursor of amyloid protein in Alzheimer disease undergoes fast anterograde axonal transport. *Proc. Natl. Acad. Sci. USA* **87**, 1561-1565.

Koo, E. H., Squazzo, S. L., Selkoe, D. J. and Koo, C. H. (1996). Trafficking of cell-surface amyloid beta-protein precursor. I. Secretion, endocytosis and recycling as detected by labeled monoclonal antibody. *J. Cell Sci.* **109**, 991-998.

Kuhn, P.-H., Wang, H., Dislich, B., Colombo, A., Zeitschel, U., Ellwart, J. W., Kremmer, E., Roßner, S. and Lichtenthaler, S. F. (2010). ADAM10 is the physiologically relevant, constitutive alpha-secretase of the amyloid precursor protein in primary neurons. *EMBO J.* **29**, 3020-3032.

Lammich, S., Kojro, E., Postina, R., Gilbert, S., Pfeiffer, R., Jasionowski, M., Haass, C. and Fahrenholz, F. (1999). Constitutive and regulated alpha-secretase cleavage of Alzheimer's amyloid precursor protein by a disintegrin metalloprotease. *Proc. Natl. Acad. Sci. USA* **96**, 3922-3927.

Lasiecka, Z. M. and Winckler, B. (2011). Mechanisms of polarized membrane trafficking in neurons – focusing in on endosomes. *Mol. Cell. Neurosci.* **48**, 278-287.

Lazarov, O., Morfini, G. A., Lee, E. B., Farah, M. H., Szodorai, A., DeBoer, S. R., Koliatsos, V. E., Kins, S., Lee, V. M., Wong, P. C. et al. (2005). Axonal transport, amyloid precursor protein, kinesin-1, and the processing apparatus: revisited. *J. Neurosci.* **25**, 2386-2395.

Ludwig, A., Blume, J., Diep, T. M., Yuan, J., Mateos, J. M., Leuthäuser, K., Steuble, M., Streit, P. and Sonderegger, P. (2009). Calsyntenins mediate TGN exit of APP in a kinesin-1-dependent manner. *Traffic* **10**, 572-589.

Marquez-Sterling, N. R., Lo, A. C., Sisodia, S. S. and Koo, E. H. (1997). Trafficking of cell-surface beta-amyloid precursor protein: evidence that a sorting intermediate participates in synaptic vesicle recycling. *J. Neurosci.* **17**, 140-151.

Matsuda, S., Matsuda, Y. and D'Adamio, L. (2003). Amyloid beta protein precursor (AbetaPP), but not AbetaPP-like protein 2, is bridged to the kinesin light chain by the scaffold protein JNK-interacting protein 1. *J. Biol. Chem.* **278**, 38601-38606.

Maxfield, F. R. and McGraw, T. E. (2004). Endocytic recycling. *Nat. Rev. Mol. Cell Biol.* **5**, 121-132.

McLoughlin, D. M., Standen, C. L., Lau, K. F., Ackerley, S., Bartnikas, T. P., Gitlin, J. D. and Miller, C. C. (2001). The neuronal adaptor protein X11alpha interacts with the copper chaperone for SOD1 and regulates SOD1 activity. *J. Biol. Chem.* **276**, 9303-9307.

Miller, C. C., McLoughlin, D. M., Lau, K. F., Tennant, M. E. and Rogelj, B. (2006). The X11 proteins, Abeta production and Alzheimer's disease. *Trends Neurosci.* **29**, 280-285.

Morfini, G., Szebenyi, G., Elluru, R., Ratner, N. and Brady, S. T. (2002). Glycogen synthase kinase 3 phosphorylates kinesin light chains and negatively regulates kinesin-based motility. *EMBO J.* **21**, 281-293.

Murayama, K. S., Kametani, F., Saito, S., Kume, H., Akiyama, H. and Araki, W. (2006). Reticulons RTN3 and RTN4-B/C interact with BACE1 and inhibit its ability to produce amyloid beta-protein. *Eur. J. Neurosci.* **24**, 1237-1244.

Muresan, V., Varvel, N. H., Lamb, B. T. and Muresan, Z. (2009). The cleavage products of amyloid-beta precursor protein are sorted to distinct carrier vesicles that are independently transported within neurites. *J. Neurosci.* **29**, 3565-3578.

Nitsch, R. M., Slack, B. E., Wurtman, R. J. and Growdon, J. H. (1992). Release of Alzheimer amyloid precursor derivatives stimulated by activation of muscarinic acetylcholine receptors. *Science* **258**, 304-307.

Perez, R. G., Soriano, S., Hayes, J. D., Ostaszewski, B., Xia, W., Selkoe, D. J., Chen, X., Stokin, G. B. and Koo, E. H. (1999). Mutagenesis identifies new signals for beta-amyloid precursor protein endocytosis, turnover, and the generation of secreted fragments, including Abeta42. *J. Biol. Chem.* **274**, 18851-18856.

Rajendran, L., Honsho, M., Zahn, T. R., Keller, P., Geiger, K. D., Verkade, P. and Simons, K. (2006). Alzheimer's disease beta-amyloid peptides are released in association with exosomes. *Proc. Natl. Acad. Sci. USA* **103**, 11172-11177.

Rajendran, L., Schneider, A., Schlechtingen, G., Weidlich, S., Ries, J., Braxmeier, T., Schwille, P., Schulz, J. B., Schroeder, C., Simons, M. et al. (2008). Efficient inhibition of the Alzheimer's disease beta-secretase by membrane targeting. *Science* **320**, 520-523.

Roghani, M., Becherer, J. D., Moss, M. L., Atherton, R. E., Erdjument-Bromage, H., Arribas, J., Blackburn, R. K., Weskamp, G., Tempst, P. and Blobel, C. P. (1999). Metalloprotease-disintegrin MDC9: intracellular maturation and catalytic activity. *J. Biol. Chem.* **274**, 3531-3540.

Rusu, P., Jansen, A., Soba, P., Kirsch, J., Löwer, A., Merdes, G., Kuan, Y. H., Jung, A., Beyreuther, K., Kjaerulff, O. et al. (2007). Axonal accumulation of synaptic markers in APP transgenic Drosophila depends on the NPTY motif and is paralleled by defects in synaptic plasticity. *Eur. J. Neurosci.* **25**, 1079-1086.

Sisodia, S. S. (1992a). Beta-amyloid precursor protein cleavage by a membrane-bound protease. *Proc. Natl. Acad. Sci. USA* **89**, 6075-6079.

Sisodia, S. S. (1992b). Secretion of the beta-amyloid precursor protein. *Ann. N. Y. Acad. Sci.* **674**, 53-57.

Slack, B. E., Ma, L. K. and Seah, C. C. (2001). Constitutive shedding of the amyloid precursor protein ectodomain is up-regulated by tumour necrosis factor-alpha converting enzyme. *Biochem. J.* **357**, 787-794.

Small, S. A. and Gandy, S. (2006). Sorting through the cell biology of Alzheimer's disease: intracellular pathways to pathogenesis. *Neuron* **52**, 15-31.

Steuble, M., Gerrits, B., Ludwig, A., Mateos, J. M., Diep, T. M., Tagaya, M., Stephan, A., Schätzle, P., Kunz, B., Streit, P. et al. (2010). Molecular characterization of a trafficking organelle: dissecting the axonal paths of calsyntenin-1 transport vesicles. *Proteomics* **10**, 3775-3788.

Szodorai, A., Kuan, Y. H., Hunzelmann, S., Engel, U., Sakane, A., Sasaki, T., Takai, Y., Kirsch, J., Müller, U., Beyreuther, K. et al. (2009). APP anterograde transport requires Rab3A GTPase activity for assembly of the transport vesicle. *J. Neurosci.* **29**, 14534-14544.

Tienari, P. J., De Strooper, B., Ikonen, E., Simons, M., Weidemann, A., Czech, C., Hartmann, T., Ida, N., Multhaup, G., Masters, C. L. et al. (1996). The beta-amyloid domain is essential for axonal sorting of amyloid precursor protein. *EMBO J.* **15**, 5218-5229.

Torroja, L., Packard, M., Gorczyca, M., White, K. and Budnik, V. (1999). The Drosophila beta-amyloid precursor protein homolog promotes synapse differentiation at the neuromuscular junction. *J. Neurosci.* **19**, 7793-7803.

Vagnoni, A., Perkinton, M. S., Gray, E. H., Francis, P. T., Noble, W. and Miller, C. C. J. (2012). Calsyntenin-1 mediates axonal transport of the amyloid precursor protein and regulates Aβ production. *Hum. Mol. Genet.* **21**, 2845-2854.

Vassar, R. (2004). BACE1: the beta-secretase enzyme in Alzheimer's disease. *J. Mol. Neurosci.* **23**, 105-114.

Vogt, L., Schrimpf, S. P., Meskenaite, V., Frischknecht, R., Kinter, J., Leone, D. P., Ziegler, U. and Sonderegger, P. (2001). Calsyntenin-1, a proteolytically processed postsynaptic membrane protein with a cytoplasmic calcium-binding domain. *Mol. Cell. Neurosci.* **17**, 151-166.

Weskamp, G., Cai, H., Brodie, T. A., Higashyama, S., Manova, K., Ludwig, T. and Blobel, C. P. (2002). Mice lacking the metalloprotease-disintegrin MDC9 (ADAM9) have no evident major abnormalities during development or adult life. *Mol. Cell. Biol.* **22**, 1537-1544.

Yamashiro, D. J., Fluss, S. R. and Maxfield, F. R. (1983). Acidification of endocytic vesicles by an ATP-dependent proton pump. *J. Cell Biol.* **97**, 929-934.

Yamazaki, T., Koo, E. H. and Selkoe, D. J. (1996). Trafficking of cell-surface amyloid beta-protein precursor. II. Endocytosis, recycling and lysosomal targeting detected by immunolocalization. *J. Cell Sci.* **109**, 999-1008.